

OFDMA-BASED NETWORKS CAPACITY IMPROVEMENT USING ENHANCED FRACTIONAL FREQUENCY REUSE SCHEME

OMAR M. ESHANTA, MAHAMOD ISMAIL, ROSDIADEE NORDIN, NOR FADZILAH A

Faculty of Engineering, Universiti Kebangsaan Malaysia

E-mail: omarshanta@gmail.com, mahamod@ukm.edu.my, adee@ukm.edu.my, fadzilah.abdullah@ukm.edu.my

ABSTRACT

OFDMA as a broadband technology is intended to offer high data rate services. In cellular networks, a Frequency Reuse (FR) principle has been used to maximize the Signal to Noise-plus-Interference Ratio (SINR), which in turn allows high data rates and spectral efficiency to be achieved. Earlier FR schemes used in 2G and 3G networks are known as Integer Frequency Reuse (IFR) schemes, and were able to improve the global SINR of the system but not the interference at cell edge. Fractional Frequency Reuse (FFR) schemes have been proposed in OFDMA based networks (WiMAX forum 2006) to combat the low SINR at cell edge and gain more amount of spectrum per cell. The tradeoff between interference mitigation using IFR schemes and the extra cell BW gained from FFR scheme needs to be considered. There is a need for the analysis and optimization of FFR key parameters which control the system performance to ensure the highest data rate and spectral efficiency. In this paper, we propose a new FFR-based scheme called Enhance FFR (EFFR), deriving its analytic model and using simulations to evaluate its performance along with different FR schemes and patterns, including IFR and FFR (classified into Hard, HFFR and Soft, SFFR). The effective SINR ($SINR_{eff}$) and Cell Data Rate (DR_{cell}) are used as performance criteria. Further, the optimum values of $SINR_{th}$ and power ration ψ have been defined for all FR patterns. Simulation results show that the highest DR_{cell} was obtained from the proposed EFFR 1x3x3, followed by SFFR 3x1x1, at 137.85 Mbps and 111.33 Mbps, respectively.

Keywords: OFDMA, Fractional Frequency Reuse FFR, Frequency Reuse Schemes, Spectral Efficiency

1. INTRODUCTION

In wireless communications systems, to improve the usability of the available spectrum the total frequency band is divided into sub bands that are allocated to adjacent divisions of the system area. This technique can reduce the overall system Signal to Interference plus Noise Ratio $SINR$, hence improves the capacity. However, the Cell Edge Users (CEU) still suffer from high levels of interference and low $SINR$. This case is called Integer Frequency Reuse (IFR), as shown in Figure 1. To solve the problem of low $SINR$ at CEU, a technique called Fractional Frequency Reuse (FFR) has been introduced. FFR divides the cell area into inner and outer areas and uses different Frequency Reuse Factor (FRF) for each one with power level of the outer area higher than that used in IFR. For example, the inner area can have $FRF = 1$, while the outer area has $FRF = 3$.

Investigation and optimization of FFR control parameters (i.e., power ratio and $SINR$ threshold), is an interesting challenge that is being considered by researchers. Only few works have focused on finding the optimum Frequency Reuse Scheme (FRS) and the optimum values of their parameters; however, not all FRS patterns have been considered and the optimal values of such parameters have been determined independently.

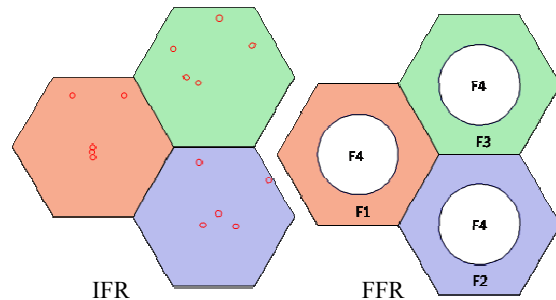


Figure 1: FRS in OFDMA-based systems

The work in this paper contributes to the improvement of OFDMA-based networks' capacity by proposing a new FFR scheme that improves the total cell data rate with acceptable spectral efficiency. This is achieved by sectorizing the Cell Center Area (CCA) and Cell Edge Area (CEA) and allocating different sub-bands to the sectors of the same angle, reducing interference and increase total cell BW. We further employ simulation modeling to investigate and analyze various FFR schemes including HFFR and SFFR and to determine its optimum pattern and values for the $SINR_{th}$ and power ratio parameters.

The rest of the paper is organized as follows. Section 2 elaborates on the most relevant works, while Section 3 introduces the basic idea of the proposed FFR scheme. Section 4 an analytical model is derived to facilitate the simulations, for which a corresponding model is presented in Section 5. The results of the simulations are discussed in Section 6, whereas the paper is concluded in Section.

2. RELATED WORK

Investigation and analysis of Frequency Reuse Schemes (FRS) has been addressed in some works in literature. Some of them aimed to analyze and evaluate the different FR scenarios, others worked on determining the optimal values of system parameters. Most of these works considered the standardized frequency reuse patterns of IFR and FFR. However, the different patterns of SFFR and HFFR have not been addressed sufficiently, which leaves room for more extensive investigations. Hereafter the most related works are being presented.

Yuefeng et al. [1] provide a quantitative analysis using system level simulation with two tiers wrap around to investigate the performance of Down Link (DL) FFR in WiMAX networks. The performance of the FFR schemes with sectorized and none sectorized cell layout was investigated in terms of throughput and cell coverage. The FRSs considered in their simulations are, frequency reuse one, frequency reuse three with segmentation, and FFR with different reuse zone size split. Simulation results showed that using frequency reuse one the ICI will be decreased and hence the coverage will be degraded. To improve the $SINR$ a FR 3 can be used and the coverage will be improved as well. However, using FR 3 decreases the cell throughput since only 1/3 of the resources (subchannels) is assigned to each sector. The solution to this tradeoff

between coverage and throughput is the FFR. According to the simulation results, FFR scheme can maintain the coverage of FR 3 with an improvement of the throughput at the same time. This work proved the possibility of improving the spectral efficiency of OFDMA-based networks using FFR scheme.

Another author in the same year [2] has determined the optimal FR factor of the Cell Edge Users (CEU) as well as the allocated resources to both inner and outer zones of FFR scheme that meets the highest QoS (cell throughput). The author used a system layout of 18 cells and 40 users per cell, distributed uniformly, and assumed a flat fading channel with adjacent subcarrier allocation. The problem had been formulated as an optimization problem, and was solved by Primal Dual Interior Point Method. Results showed that the best configuration that meets the highest throughput is achieved with FRF = 3 for CEU and by allocating 32 chunks (group of 12 subcarriers) to the inner cell region and 18 chunks to be shared among 3 neighbor cells. The optimal inner cell radius was determined and was approximately equal to 2/3 of the overall cell radius. The results of this work are worthy and quite precise; however, the assumptions of adjacent subcarrier allocation with flat fading channel are more suitable for fixed wireless networks, but not mobile wireless networks which are frequency selective and employ distributed subcarrier allocation to gain frequency diversity.

One of the most related works was by Masood [3]. Besides the valuable outcomes of his work including the analysis and investigation of permutation schemes and adaptive beam forming technique, the author extensively investigated and compared the performance of FRS including six IFR patterns and two FFR patterns, namely FFR and Two Level Power Control (TLPC). Even though the FFR principle has not been standardized yet at the time of Masood's work, his results and analysis are considered a very good input to evaluate the OFDMA system performance under such scenarios. In his work on FRS, the author considered three different scheduling schemes, namely: equal data rate, equal bandwidth and opportunistic. Based on a fluid model that was originally proposed for CDMA networks, Masood proposed an analytical model for IFR, FFR, and TLPC schemes in terms of SIR and total cell data rate. A comparison between the above mentioned FRS and scheduling policies in terms of SIR and



cell throughput was carried out, and optimal values of FFR parameters, namely inner cell radius and power ratios were proposed.

The two main types of FFR namely strict (hard) FFR and soft frequency reuse (SFR) have been evaluated and compared in [4]. Several evaluation metrics have been used, including outage probability, spectral efficiency, network throughput, and average CEU *SINR*. In their simulation, the authors considered the path loss and small-scale fading (fast fading) for simplicity. They also considered a Base Station (BS) with the same transmitted power for strict FFR (HFFR) and power ratio $\beta \geq 1$ ($\beta = P_{out} / P_{in}$) for SFR (SFFR). The users have been classified as CEU or CCU by calculating the average *SINR* and compared with a predetermined threshold (*SINR_{th}*). The resources were allocated proportionally to the inner and outer radii (*R_{in}* / *R_{out}*), which varies with *SINR_{th}*. The results of this work showed that the strict FFR outperforms the SFR in terms of outage probability and it is less sensitive to the *R_{in}* than SFR. However, by increasing the power ratio factor (β) SFR can show improvement in outage probability. From network throughput point of view, strict FFR shows the greatest performance and achieves the highest CEU *SINR* compared to SFR; on the other hand, SFR provides the balance between the interference reduction and efficiency of resource allocation.

Another work [5] presented a new analytical framework to evaluate the coverage probability and average rate in the two scenarios of strict and soft FFR, instead of evaluating the two cases through system level simulations. Moreover, they proposed a resource allocation strategy that allocates the sub bands proportional to the average *SINR*. An important conclusion from their results was to show how the power control factor β influences the *SINR* of CEU. Their results showed that as β increases the *SINR* and hence the probability of coverage of CEU increases. At $\beta=15$, the performance of SFR approaches and then exceeds the performance of strict FFR. However, the performance of SFR in terms of *SINR* and coverage probability is bounded by two limits; lower bound, when $\beta = 1$ for FR 1, and upper bound when β tends to infinity for FRF > 1. The performance of the two scenarios in terms of data rate follows the previous conclusion, whereas the strict FFR outperforms the SFR until β approaches 15 where the data rate of SFR reaches and then exceeds the data rate of strict FFR. Another factor

that plays a big role in the FFR system is the initial *SINR* threshold (denoted by TFR) which classifies the users into CEU and CCE. Results showed that, as TFR increases, the average data rate also increases, as the low *SINR* users will be transferred to the CEU region with a higher power factor, which will improve their *SINR* and hence the data rate. However, this threshold has an optimal value, whereby exceeding this optimal value the average cell- data rate starts to decrease, this optimal TFR had not been defined precisely in this work. In general, both strict FFR and SFR schemes outperform the IFR scheme. The cell data rate increases as β increases, while TFR has an optimal value, which meets the highest performance.

Yet another work by Hamza [6] comprehensively surveyed the various Inter-Cell Interference Coordination (ICIC) schemes in the downlink of OFDMA-based cellular networks. The authors used smart notations to classify and categorize various static (frequency reuse-based) and dynamic (cell coordination-based) ICIC schemes. The FFR itself was divided into three classes. First class is Partial Frequency Reuse (PFR), also known in the literature as Strict FFR or HFFR; PFR implements Frequency Reuse Factor (FRF) of 1 in Cell Center (CC) and FRF of 3 in the Cell Edge (CE). The second class is Soft Frequency Reuse (SFR) which implements FRF > 1 in CC and FRF = 3 in the CE with two power levels. The last class is Intelligent Frequency Reuse, which allocates the frequency bands to different sectors based on the load distribution, so it can start with FRF 3 if there is no much load on CE, PFR, SFR, or even Integer FR (IFR) with FRF = 1 in high offered load. Another spectrally efficient scheme that was surveyed in this work is called Enhanced FFR (EFFR). EFFR divides the frequency band into two segments, primary segment which is unique for each cell and secondary segment which is common with neighboring cells in non sectorized and FRF = 3 system. The users are allowed to use their own primary segment, but they need to negotiate with neighboring to use the secondary segment. Besides the wide presentation of the various FFR schemes, the authors presented a conclusion from their work and other's work stating the most important parameters that affect the performance of networks that employ FFR schemes.

3. PROPOSED EFFR SCHEME

As a general conclusion from the above related works, particularly [3], [5], and [6], the FFR principle can significantly increase the *SINR* of

CEU; hence improve the spectral efficiency of the system. The power control factor (the power ratio) and the SINR threshold are the most important parameters that play a big role in the system performance; also the system layout and the FR pattern have a significant impact on the cell data rate and hence on the spectral efficiency. This conclusion gave the motivation to explore and expand these works in order to include more options and scenarios and to come out with new findings.

We start by presenting the proposed Enhanced FFR (EFFR) scheme that improves the performance of FFR scheme. The principle is to reduce the interference and increase total cell BW by sectorizing the Cell Center Area (CCA) and Cell Edge Area (CEA), and to allocate different subbands to the sectors of the same angle as shown in Figure 2. The advantage of this scheme consists of:

- i. Sectorization of CCA reduces the interference compared to HFFR and SFFR.
- ii. The entire BW is allocated to CEA and reallocated to CCA, which means 200% of total available BW.
- iii. Using two power levels for CCA and CEA; this reduces total transmitted power and interference.

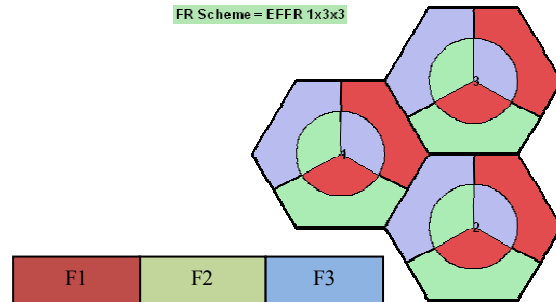


Figure 2: Proposed EFFR cell layouts

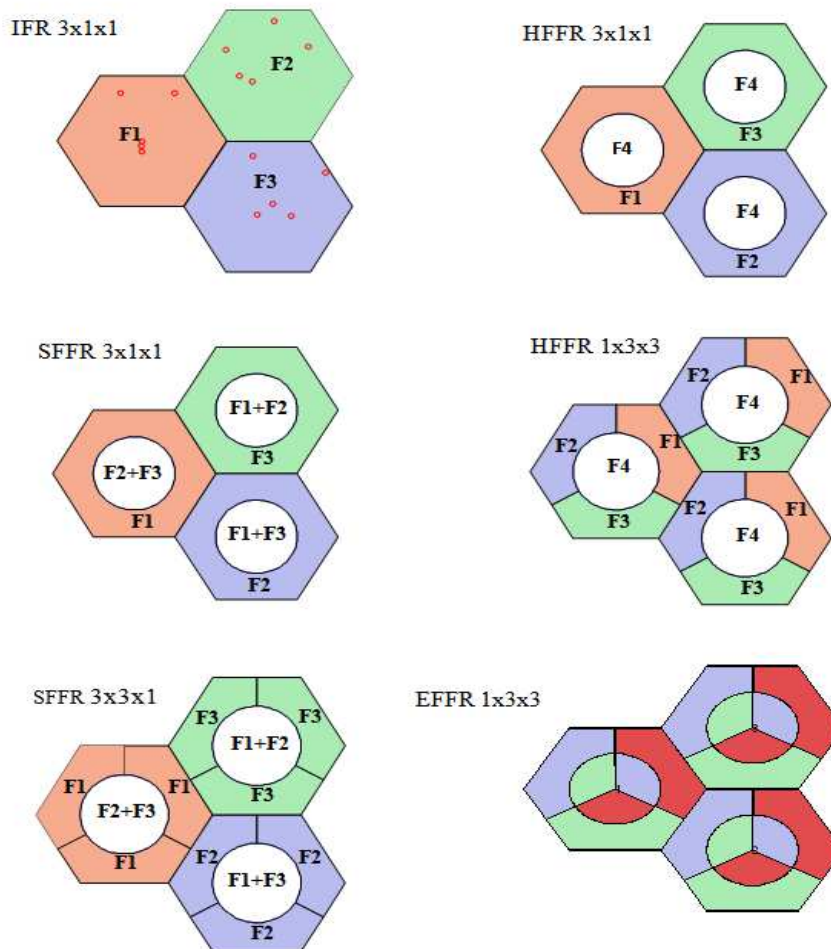


Figure 3: OFDMA FRs with various patterns and sub bands allocation

4. ANALYTICAL MODEL

In this section, the analytical model, which includes the calculations of power and interference, per subcarrier *SINR*, effective *SINR*, and cell data rate, are derived to facilitate the simulations and analysis of OFDMA based networks with various FRs and FR patterns. The patterns covered in this analysis are shown in Figure 3.

The following assumptions are adopted throughout all of our analysis and simulations:

- i. A multi-cell and multi-user OFDMA based system with PUSC permutation scheme.
- ii. Regardless of the number of MSs, A fully utilized spectrum is being assumed.
- iii. The available spectrum is divided into three or four equal sub-bands (depending on the FR pattern used) as in Figure 3.

4.1 Propagation Model

According to WiMAX Forum [7], the extended COST-231 HATA model has been recommended for system simulations and network planning of macro cellular systems in both urban and suburban areas for mobility applications. The model is formulated as follows:

$$L_{50}(\text{urban}) = 46.3 + 33.9 \log f_c - 13.82 \log ht - a(hr) + (44.9 - 6.55 \log h_t) \log d + C_m \quad (1)$$

where:

$C_m = 0\text{dB}$ for suburban areas, and 3dB for metropolitan centers;

f_c : operating frequency from 1500 - 2000 MHz;

h_t : transmitter antenna height 30 - 200 meters;

h_r : receiver antenna height 1 - 10 meters;

d : distance 0.1 - 20 km;

$a(hr) = 3.2(\log(11.75hr))^2 - 4.97$, for suburban environment;

$a(hr) = (1.1 \log(fc) - 0.7)hr - (1.56 \log(fc) - 0.8)$, for urban environment

The channel of OFDMA based networks with 20 MHz BW over single subcarrier can be considered a flat fading channel. Since the frequency spacing between subcarriers is 10.94 kHz, with delay spread of 10 μs (normally it ranges from 100 ns to 10 μs), then the coherence bandwidth is about 100 kHz, which spans more than 8 subcarriers. However, over a 24 subcarriers (one subchannel) the channel is considered as frequency selective channel. So, in our simulation, the slow fading will be updated every subchannel,

whereas fast fading is calculated for every subcarrier.

4.2 Interference Modeling

In multi carrier systems, individual subcarrier may have various experiences of channel gain and interference. This variance increases in OFDMA based systems, where the resource units allocated to MSs consist of spectrally disjoint subcarriers. Thus a per subcarrier power, interference, and SINR need to be modeled.

Assuming a fully loaded system without using power control, the total power transmitted by BS (P_{BS}) will be divided evenly among the N subcarriers allocated to such BS, so the per subcarrier power (P_{SC}) can be expressed as:

$$P_{SC} = P_{BS} / N \quad (2)$$

However, N is not same for all FR patterns and depends on the number of sectors and the intra-cell FRF. Using FR pattern notations ($N_c \times N_t \times N_f$), N can be expressed as follows:

$$N = \begin{cases} \frac{N_t N_{Sc}}{N_f} & \text{for sectorized cells} \\ \frac{N_t N_{Sc}}{N_c} & \text{for non-sectorized cells} \end{cases} \quad (3)$$

where N_c is the number of cells in the network cluster (it determines the inter-cellular frequency reuse), N_t is the number of sectors in a cell, N_f is intra-cellular frequency reuse and N_{Sc} is the total number of subcarriers (data + pilot) allocated to the BS in the case of FRF of one.

Interference modeling of FFR scheme is different from IFR scheme where all MSs within the serving cell experience interference from all other cells in the grid. In FFR scheme, according to the FR pattern, MSs may experience interference from part of the cells. Additionally, if two power levels have been used, different locations of MSs will experience different interference with different power levels. Moreover, in some FR patterns, a MS may experience interference on different subcarriers with two power levels from the same BS. Thus, defining an interference model for different FR patterns is necessary.

First of all, we classify the MSs based on their location into, Cell Center User (CCU) for MSs located within the Cell Center Area (CCA) and Cell

Edge User (CEU) for MSs located within Cell Edge Area (CEA). Also, we define two sets of interferers; I_{CCA} represents the set of BSs that interfere with MSs located within CCA and I_{CEA} represents the set of BSs that interfere with MSs located within CEA. The two power levels are denoted by P_{CCA} and P_{CEA} as shown in Table 1.

Table 1: Defining the set of interferers (I_{CCU} and I_{CEU}) for each FRS.

FR pattern	I_{CCA}	I_{CEA}
IFR (3x1x1)	NA	$P_{CEA}\{9,11,13,15,17,19\}$
HFFR (3x1x1)	$P_{CCA}\{2:19\}$	$P_{CEA}\{9,11,13,15,17,19\}$
SFFR (3x1x1)	$P_{CCA}\{3,5,7,8,9,11,12,13,15,16,17,19\}$ $P_{CEA}\{3,5,7,8,12,16\}$	$P_{CCA}\{2:7,8,10,12,14,16,18\}$ $P_{CEA}\{9,11,13,15,17,19\}$
SFFR (3x3x1)	$P_{CCA}\{3,5,7,8,9,11,12,13,15,16,17,19\}$ $P_{CEA}\{3,5,7,8,12,16\}$	$P_{CCA}\{2:7,8,10,12,14,16,18\}$ $P_{CEA}\{9,11,13,15,17,19\}$
HFFR (1x3x3)	$P_{CCA}\{2:19\}$	$P_{CEA}\{5,6,7,14,15,16,17,18\}$
EFFR (1x3x3)	$P_{CCA}\{5,6,7,14:18\}$ $P_{CEA}\{2,3,8,9,10,19\}$	$P_{CCA}\{3,4,10:13\}$ $P_{CEA}\{5,6,7,14:18\}$

The power ratio between CCA and CEA is defined as: $\psi = \frac{P_{CCA}}{P_{CEA}}$. Then, the total interference

$I_{u,j}^n$ of MS u on subcarrier n from BS j can be expressed as:

$$I_{u,j}^n = P_{CEA} \left(\psi \sum_{j \in I_{CCU}} g_{u,j}^n + \sum_{j \in I_{CEU}} g_{u,j}^n \right) \quad (4)$$

where g is the channel gain between MS u and BS j , which is defined as:

$$g_{u,j}^n = SF_{u,j}^n FF_{u,j} PL(d_{u,j}) \quad (5)$$

where $SF_{u,j}^n$ and $FF_{u,j}$ represent the Slow Fading (log-normal) and Fast Fading (Rayleigh) factors, respectively; PL is the path loss (COST-HATA-231, suburban), and $d_{u,j}$ is the distance between MS u and BS j .

4.3 Subcarrier SINR Modeling

Taking into account the thermal noise, path loss, Fast Fading (FF), and Slow Fading (SF), the $SINR$ per subcarrier can be expressed as follows:

$$SINR_{u,i}^n = \frac{P_{s,i} g_{u,i}^n}{\Delta f N_o + I_{u,j}^n} \quad (6)$$

where $SINR_{u,i}^n$ is the signal to interference plus noise ratio of subcarrier n over the link of user u served by base station i . Δf is the subcarrier frequency spacing, and N_o is the thermal noise density. Table 2 lists the simulation parameters used in this work. These values are mainly based on [8].

Table 2: Description and values of parameters used in the simulations

Parameter	Description	Value
f	Carrier frequency	2.5 GHz
P_{BS}	Total rms transmit power of a cell	43 dBm
$N_{Sch/Slot}$	Number of Sch per Slot	2
$N_{Sc/Sch}$	Number of Sc per Sch	24
$DL:UL$	DL to UL OFDMA symbols' ratio	2:1
BW	System bandwidth	20 MHz
$FFT\ Size$	Total number of available subcarriers with Bandwidth (BW)=20MHz	2048
N_{Sc}	Total number of used subcarriers (data + pilot) corresponding to BWT	1260
N_{Sch}	Total number of used subchannels	60
σ_{SH}	Log normal shadowing standard deviation	9 dB
Δf	Subcarrier spacing	10.9375 KHz
T_s	OFDMA useful symbol duration	91.43 μ s
T_f	Frame duration	5 ms
h_{BS}	Height of BS	32 m
h_{MS}	Height of MS	1.5 m

4.4 Effective SINR Calculation

As direct averaging fails to tackle the variation of $SINR$ per subcarrier over a frequency selective channel; a method called Mean Instantaneous Capacity (MIC) [7] has been used to predict the link layer performance in a computationally simple way. In the MIC, the $SINR$ of n^{th} subcarrier is first used to calculate the instantaneous Shannon capacity of the subcarrier:

$$C_n = \log_2(1 + SINR_n) \quad [b/s/Hz] \quad (7)$$

Then using the values of capacity in Equation 3, MIC is computed by averaging capacities of N' subcarriers:



$$MIC = \frac{1}{N'} \sum_{n=1}^{N'} C_n \quad [b/s/Hz] \quad (8)$$

Then, $SINR_{eff}$ is obtained from MIC value using following equation:

$$SINR_{eff} = 2^{MIC} - 1 \quad [dB] \quad (9)$$

4.5 Sections and Subsections

Assuming a fully loaded Mobile WiMAX system, with frame duration of 5 ms, and 48.6 symbols per frame, the total cell data rate (in bps) can be expressed as:

$$DR_{cell} = \frac{1}{T_f} \sum_{k=1}^{M_s} B_{slot} \quad [bps] \quad (10)$$

where T_f is the duration of Time Division Duplex (TDD) frame, and NS is the number of slots in DL

sub-frame of a cell, which depends on the FR pattern ($N_c \times N_t \times N_f$), and is expressed as follows:

$$N_s = N_{st} \times \frac{N_t}{N_f N_c} \quad (11)$$

where N_{st} is the number of slots in DL sub-frame for FR one. B_{slot} is the number of bits per slot determined by mapping the $SINR_{eff}$ values to the corresponding MCS listed in Table 3 as follows:

$$B_{slot} = b_{sym} \times CR \times N_{Sc/Sch} \times N_{Sch/slot} \quad [Bits] \quad (12)$$

where b_{sym} is the number of bits per modulation symbol, CR is coding rate, $N_{Sc/Sch}$ is the number of Sc per Sch, and $N_{Sch/slot}$ is the number of Sch per slot.

Table 3: PHY-Layer data rate at various channel bandwidths [9]

Channel bandwidth	3.5MHz	1.25MHz	5MHz	10MHz	8.75MHz[a]					
PHY mode	256 OFDM	128 OFDMA	512 OFDMA	1,024 OFDMA	1,024 OFDMA					
Oversampling	8/7	28/25	28/25	28/25	28/25					
Modulation and Code Rate	PHY-Layer Data Rate (kbps)									
	DL	UL	DL	UL	DL	UL	DL	UL	DL	UL
BPSK, 1/2	946	326	Not applicable							
QPSK, 1/2	1,882	653	504	154	2,520	653	5,040	1,344	4,464	1,120
QPSK, 3/4	2,822	979	756	230	3,780	979	7,560	2,016	6,696	1,680
16 QAM, 1/2	3,763	1,306	1,008	307	5,040	1,306	10,080	2,688	8,928	2,240
16 QAM, 3/4	5,645	1,958	1,512	461	7,560	1,958	15,120	4,032	13,392	3,360
64 QAM, 1/2	5,645	1,958	1,512	461	7,560	1,958	15,120	4,032	13,392	3,360
64 QAM, 2/3	7,526	2,611	2,016	614	10,080	2,611	20,160	5,376	17,856	4,480
64 QAM, 3/4	8,467	2,938	2,268	691	11,340	2,938	22,680	6,048	20,088	5,040
64 QAM, 5/6	9,408	3,264	2,520	768	12,600	3,264	25,200	6,720	22,320	5,600

[a] The version deployed as WiBro in South Korea

5. ANALYTICAL MODEL

Simulating a cellular network with a large number of cells is often computationally inefficient. Therefore, the simulation has been designed to consider the first two tiers of the system to form a hexagonal grid of 19 cells as shown in Figure 4. However, considering a finite size of the network area causes inaccuracy of results collected at cells of edge network (known as *edge effect*). To

mitigate the edge effect, a wraparound approach has been used [10].

The procedure of this simulation is depicted in the flowchart of Figure 5, which can be divided into the following modules:

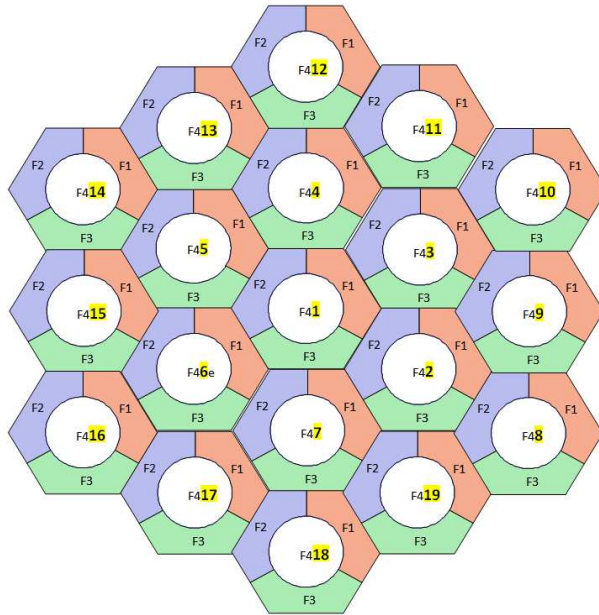


Figure 4: Cell layout

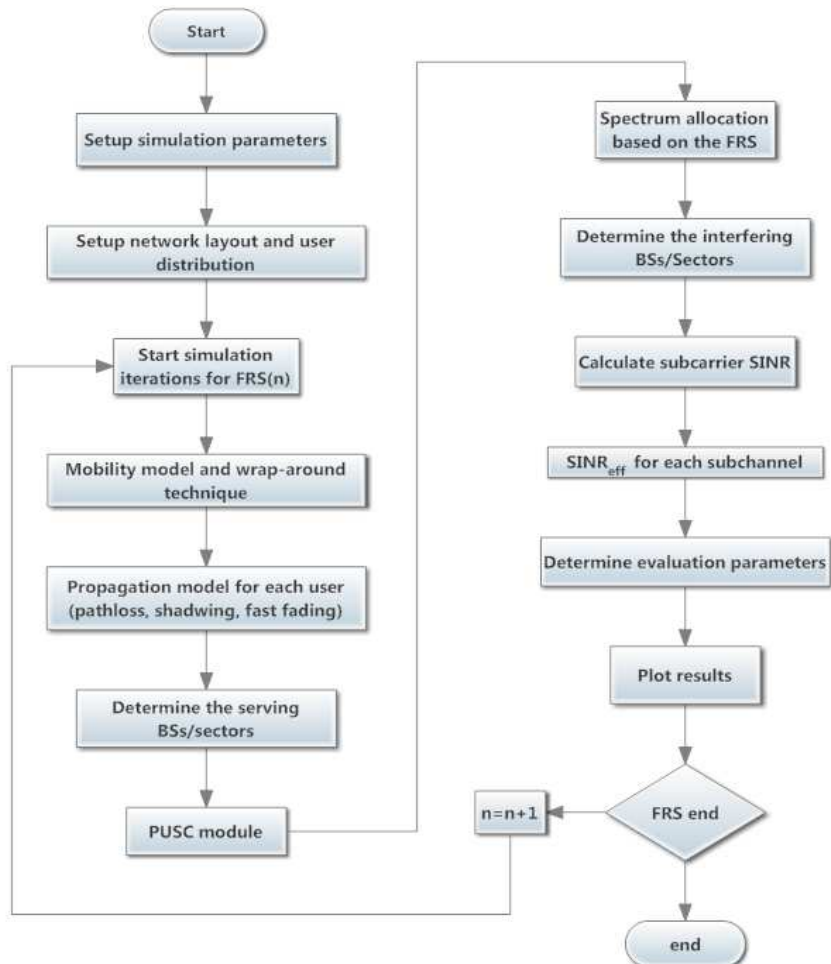


Figure 5: Simulation model

a) FR Pattern Identification Module: This module identifies the network layout parameters, such as type of FRS, IFR/FFR, cell radius, number of sectors, BW allocation for each sector/area, and the total number of users.

b) Propagation Model and MS Distribution Module: This module defines the sort of MSs' distribution over the cell area either randomly and uniformly or by defining a percentage for each sector/area. Using the maximum received signal strength, the serving BS (sector/area) will be defined to each MS.

c) Traffic Distribution Module: This module allocates the resource units to the MSs of each sector/area defined in module a, and based on a predefined type and quality of service.

6. SIMULATION RESULTS AND DISCUSSION

In this section the performance of various FFR schemes including HFFR, SFFR, and EFFR will be investigated and compared with IFR as a reference scheme. Taking $SINR_{eff}$ as performance criterion, the impact of FFR main parameters ($SINR_{th}$ and power ratio ψ) on system performance will be examined.

6.1 Sections and Subsections

Table 4 gives the BW allocation for each FR pattern where B_{CCA} and B_{CEA} are the portion of BW allocated to CCA and CEA, respectively, and B_{cell} is the total BW available for the cell ($B_{cell} = B_{CCA} + B_{CEA}$). Tables 1 and 4 will be used to facilitate the analysis and discussion of simulation results.

Table 4: Sub-band allocation for various FR patterns.

FR Pattern	B_{CCA}	B_{CEA}	B_{cell}	1x1x1%
IFR (3x1x1)	1/3 (20)	//	1/3 (20)	33%
HFFR (3x1x1)	1/4 (15)	1/4 (15)	1/2 (30)	50%
SFFR (3x1x1)	2/3 (40)	1/3 (20)	1 (60)	100%
SFFR (3x3x1)	2/3 (40)	1 (60)	5/3 (100)	167%
HFFR (1x3x3)	1/4 (15)	3/4 (45)	1 (60)	100%

Figure 6 compares the average $SINR_{eff}$ vs. distance of all FR patterns under consideration. Generally, $SINR_{eff}$ decreases with distance for all schemes. However, for FFR the $SINR_{eff}$ improves at the transition point between CCA and CEA. With $SINR_{th}$ of 20 dB and ψ of 30 %, the transition occurs at 450 meters which represents the radius of the CCA (R_{in}). Within CCA, IFR shows better performance than FFR due to the 30% less power

used for FFR schemes. When MS's $SINR_{eff}$ drops below $SINR_{th}$, it moves to CEA with 70% higher power and hence the $SINR_{eff}$ improves. The improvement in $SINR_{th}$ for each pattern depends on the amount of interference experienced. For instance, referring to the interference sets given in Table 1, SFFR shows less improvement than HFFR and the latter less than IFR.

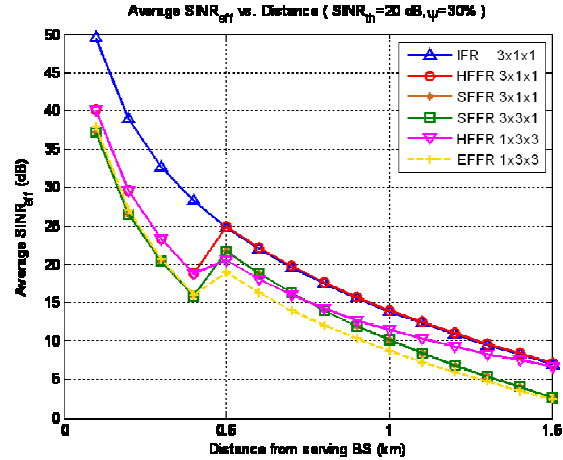


Figure 6: Effective SINR for IFR and HFFR

Generally, in a symmetrical grid of hexagonal cells with similar transmitted power from all BSs, increasing the transmitted power does not improve $SINR$ correspondingly as the interference power will be increased as well. Thus, changing the power ration of HFFR scheme will not make a remarkable effect on $SINR_{eff}$, whereas, in SFFR scheme where the interference exchanges between CCA and CEA, changing ψ can change the overall interference of the system and hence average $SINR_{eff}$ will be affected as shown in Figure 7.

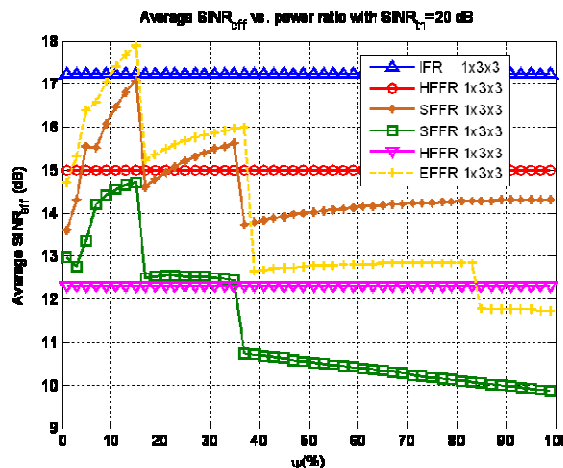


Figure 7: Impact of power ration on the average $SINR_{eff}$

The variation of average $SINR_{eff}$ vs. ψ of SFFR and EFFR schemes is determined mainly by the variation in the interference powers of I_{CCA} and I_{CEA} sets, while its amplitude is determined by the sub-bands allocation given in Table 4 as well.

Generally, excluding IFR scheme, average $SINR_{eff}$ improves with $SINR_{th}$, as shown in Figure 8. This gradual increment in average $SINR_{eff}$ can be justified due to decrement of R_{in} as $SINR_{th}$ increases, where more MSs that are closer to BS are transferred to CEA with higher power (P_{CEA}), and hence the average $SINR_{eff}$ increases.

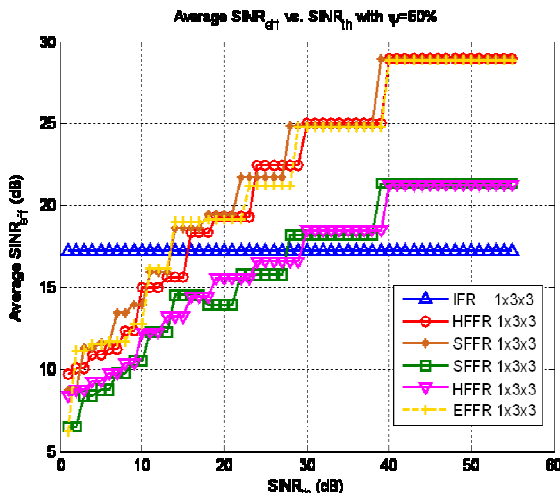


Figure 8: Impact of $SINR_{th}$ on $SINR_{eff}$ for different FR patterns

So far, the impact of ψ and $SINR_{th}$ has been examined separately. However, the full picture and the optimum values of these parameters can be obtained by considering all of them together into a single picture as presented in the next section.

6.2 Sections and Subsections

The previous section presented how the FFR scheme behaves compared to IFR, and how the FFR parameters affect the performance in terms of average $SINR_{eff}$. This section discusses the performance of FFR schemes by considering all variations of system parameters and putting them into a single picture to determine the optimal FR pattern, taking DR_{cell} as performance criterion.

The 3D plots in Figure 9 (a-f) show the variation of DR_{cell} with ψ and $SINR_{th}$ for all FR patterns under consideration.

As can be seen from the figure, HFFR scheme are not affected by power ratio as explained

earlier, whereas SFFR scheme shows a noticeable variation with ψ . On the other hand the DR_{cell} increases with $SINR_{th}$ for all FR schemes, it makes a stairs like curve with different step size due to the inconsistent variation of R_{in} as shown previously in Figure 7. Since a fully loaded system has been assumed, the subchannels allocated to each area will be redistributed evenly among the new number of MSs; some of these subchannels will be taken from MSs distant from BS and given to the new added MSs that are closer to the BS, with better $SINR_{eff}$ and higher MCS which increases the overall DR_{cell} .

The maximum DR_{cell} with 137.85 Mbps was obtained from EFFR 3x3x1 as shown in Figure 10. This improvement in DR_{cell} over other schemes is due to high BW allocation which is 200% of the total available BW (Table 4) and relatively less interferers (Table 1). SFFR 3x3x1 which has 167% of available BW comes in the second highest DR_{cell} with 111.33 Mbps. On the other hand, with equal B_{cell} , pattern SFFR 3x1x1 shows higher DR_{cell} than HFFR 1x3x3. This is because $SINR_{eff}$ in CCA where SFFR 3x1x1 has 2/3 of its total BW is higher than in CEA, and hence there is a better chance of getting higher MCS level. Table 5 gives the optimum values of $SINR_{th}$ and ψ that gives the highest DR_{cell} for each FR pattern.

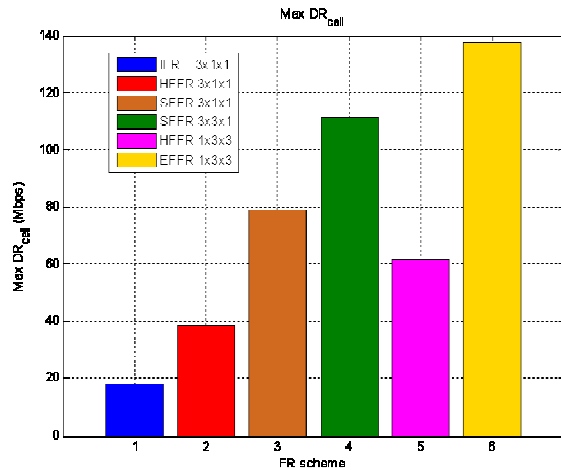


Figure 10: Comparison of maximum DR_{cell} of all FR patterns



Table 5: Optimum $SINR_{th}$ and ψ values for maximum DR_{cell}

FR pattern	Max DRcell (Mbps)	SINRth (dB)	Ψ (%)
IFR (3x1x1)	17.986	NA	NA
HFFR (3x1x1)	38.3370	40	1
SFFR (3x1x1)	78.7746	29	3
SFFR (3x3x1)	111.3348	24	3
HFFR (1x3x3)	61.7068	40	1
EFFR (1x3x3)	137.8556	25	1

7. CONCLUSION

This paper proposed a new FR scheme called EFFR to improve the system performance and spectral efficiency by offering more resources per cell. According to the simulation results, FFR scheme offers a remarkable improvement in $SINR_{eff}$ and DR_{cell} . The optimum values of $SINR_{th}$ and ψ have been defined for all FR patterns under evaluation. In addition, due to the difference in spectrum allocation and interferer sets, SFFR schemes offer better DR_{cell} than HFFR schemes. The highest DR_{cell} was obtained from EFFR 1x3x3 at 137.8556 Mbps.

8. ACKNOWLEDGMENT

We would like to express our appreciation to the reviewers for their comments; this work was supported by the government of Malaysia, e-science fund under Grant No. GGPM-2015-013.

REFERENCES:

[1] Yuefeng Zhou; Zein, Nader, 2008 "Simulation Study of Fractional Frequency Reuse for Mobile WiMAX," Vehicular Technology Conference, 2008. VTC Spring 2008. IEEE, vol., no., pp.2592, 2595, 11-14.

[2] Mohamed Assaad, 2008. "Optimal Fractional Frequency Reuse (FFR) in Multicellular OFDMA System," Vehicular Technology Conference, 2008. VTC 2008-Fall. IEEE 68th, vol., no., pp.1, 5, 21-24 Sept. 2008.

[3] Masood Maqbool, 2009 " Radio Engineering of OFDMA Access Networks ". PhD thesis. Telecom Paris Tech.

[4] Thomas Andrews, Novlan, J. G., Sohn, I., Ganti, R. K., & Ghosh, A. 2010. "Comparison of fractional frequency reuse approaches in the OFDMA cellular downlink". In GLOBECOM - IEEE Global Telecommunications Conference.

[5] Novlan, T.D.; Ganti, R.K.; Ghosh, A.; Andrews, J.G., 2011. "Analytical Evaluation of Fractional Frequency Reuse for OFDMA Cellular Networks," Wireless Communications, IEEE Transactions on, vol.10, no.12, pp.4294, 4305.

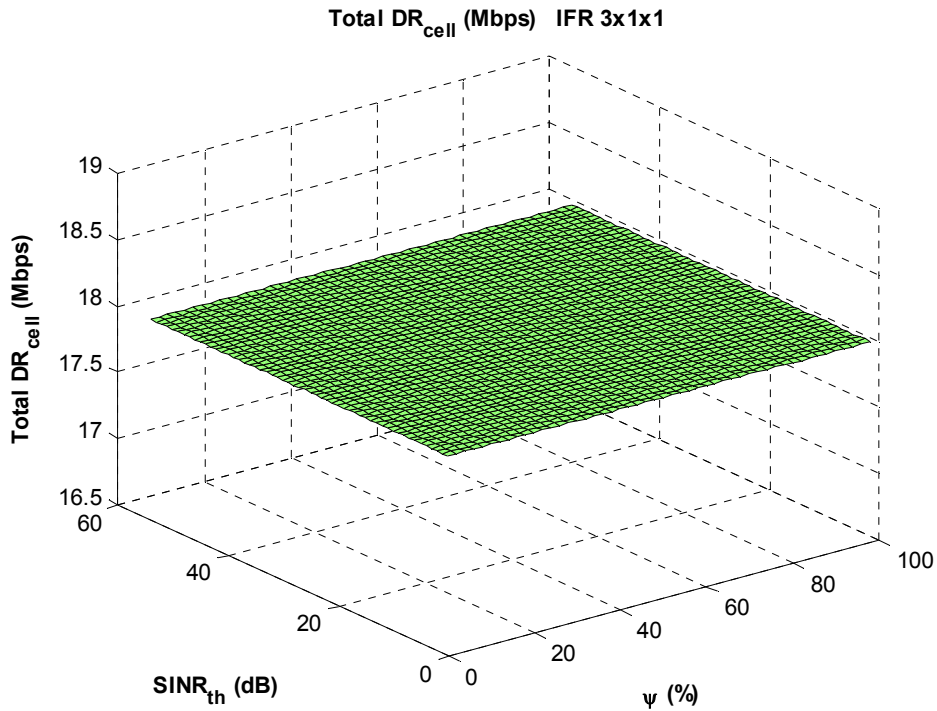
[6] Hamza, A.S.; Khalifa, S.S.; Hamza, H.S.; Elsayed, K., 2013, "A Survey on Inter-Cell Interference Coordination Techniques in OFDMA-Based Cellular Networks," Communications Surveys & Tutorials, IEEE, vol.15, no.4, pp.1642, 1670.

[7] WiMAX Forum. 2008-a. WiMAX system evaluation methodology, version 2.1.

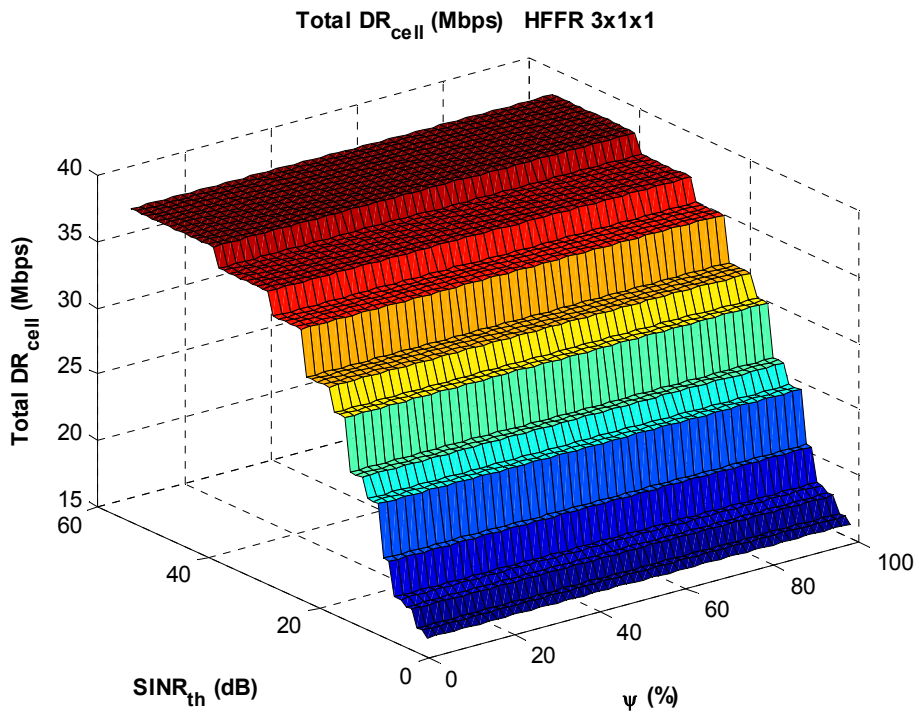
[8] Ramadas K. and Jain R. 2007. WiMAX System Evaluation Methodology, WiMAX Forum, Tech. Rep.

[9] Andrews, J.G., Ghosh, A. & Muhamed, R. 2007. Fundamentals of WiMAX: Understanding broadband wireless networking. New Jersey: Prentice Hall.

[10] David Huo. Mar 2005. "Clarification on the Wrap-Around Hexagon Network Structure", IEEE 802.20 Working Group on Mobile Broadband Wireless Access, IEEE C802.20-05/15.

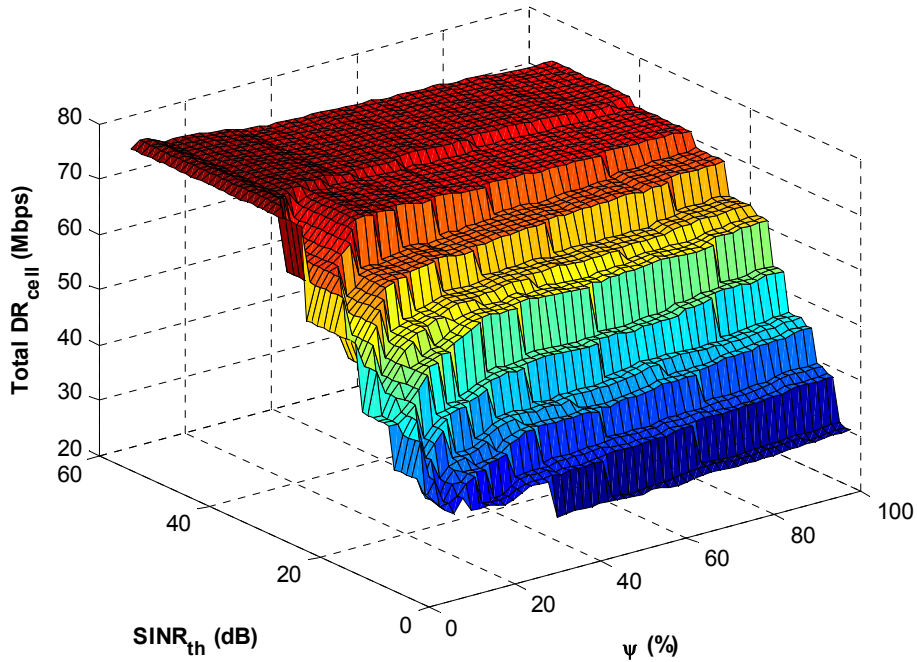


(a)



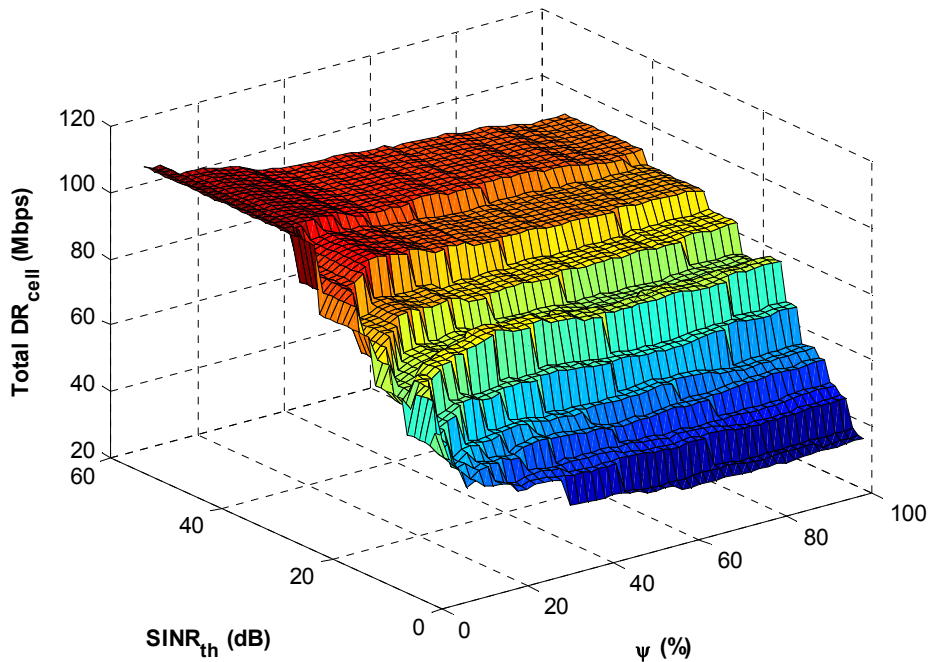
(b)

Total DR_{cell} (Mbps) SFFR 3x1x1

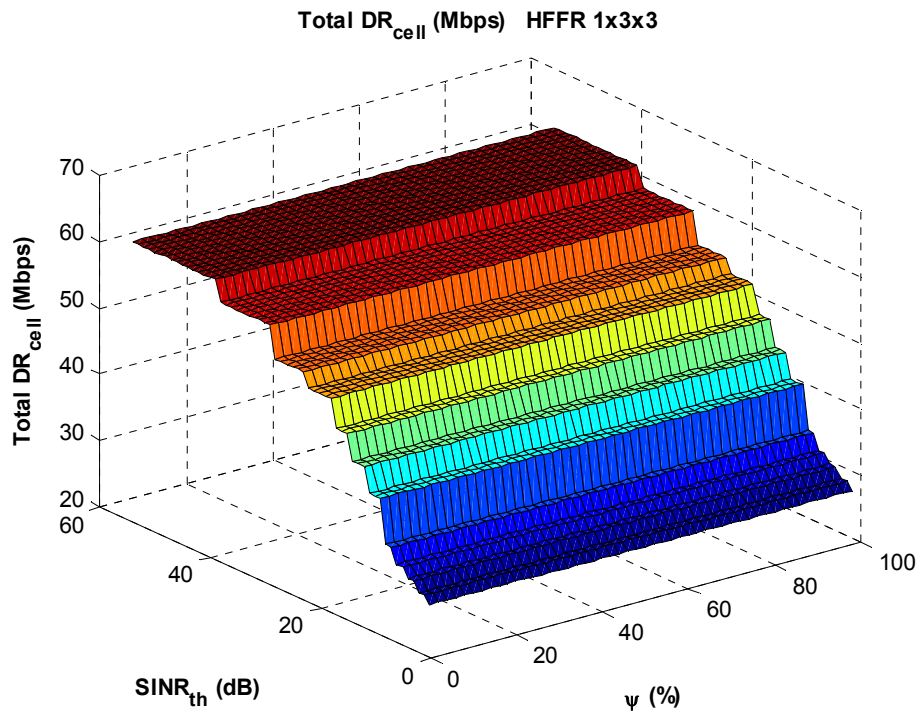


(c)

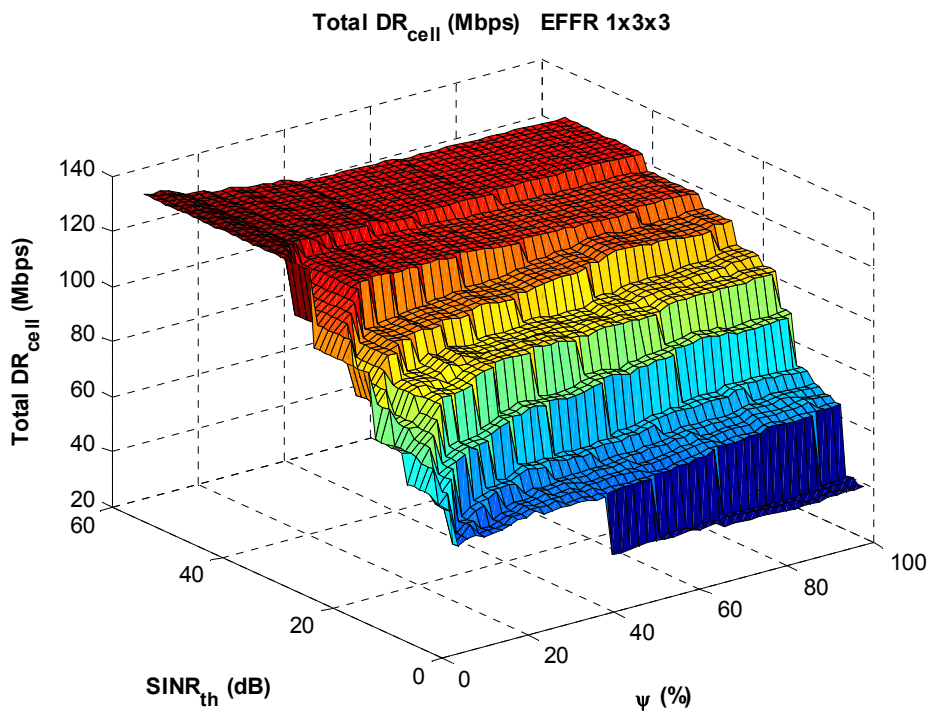
Total DR_{cell} (Mbps) SFFR 3x3x1



(d)



(e)



(f)

Figure 9 Total DR_{cell} vs. ψ and SINR_{th} for all FR schemes